

DEEP LEARNING PNN CLASSIFIER FOR DIABETIC RETINOPATHY IDENTIFICATION

Abstract

Diabetic retinopathy (DR) is a severe difficulty that requires immediate diagnosis and treatment to prevent visual loss. Lesions caused by the disorder are difficult to detect using manual approach since they appear in microscopic and subtle forms beneath the eye's structure. To address this problem, this study proposes an automated classification approach that uses Machine Learning (ML) models to evaluate the severity of DR. This automated classification approach is done followed by various image processing steps. Initially, bilateral filter is used which serves as a preprocessing tool and it is an essential step in retinal image analysis. It effectively eliminates the noise in the image by preserving the details of retinal vessels and produces an enhanced image quality for further processing. After noise removal, segmentation is done using Spatial Fuzzy C-Means (SFCM) clustering which integrates the spatial data into the membership function for clustering and generates the optimized segmented result. Following segmentation, feature extraction and feature selection is done using Gray Level Co-occurrence Matrix (GLCM) and Genetic Algorithm respectively and finally Probabilistic Neural Network (PNN) classifier is employed to detect the severity grading of DR. The results reveal that the proposed approach for identifying DR using fundus pictures of retinal is extremely efficient and effective.

Keywords: Bilateral filter, SFCM, GA, GLCM, PNN.

Authors

A Yazhini

Research Scholar
Department of Computer Science and Engineering
College of Engineering, Guindy Campus
Anna University
Chennai, Tamil Nadu, India
ayazhini55@gmail.com

S Mohanalakshmi

Professor
Department of Electronics and Communication Engineering
Rohini College of Engineering and Technology
Kanyakumari, Tamil Nadu, India
jaimohana1973@gmail.com

T Saravanan

Assistant Professor (SG)
Department of AIML
Saveetha Engineering College
Chennai, Tamil Nadu, India
saranme63@gmail.com

A. T. R Krishna Priya

PG Scholar
Department of Computer Science and Engineering
Rohini College of Engineering and Technology
Kanyakumari, Tamil Nadu, India
priya.gita6@gmail.com

I. INTRODUCTION

One of the retinal abnormalities known as diabetic retinopathy causes a diabetic patient to experience severe vision damage as an outcome of an impaired retina. The last and maximum serious stage of DR is named as Proliferative Diabetic Retinopathy (PDR). At this point, irregular and delicate blood vessels begin forming on the retina's surface [1, 2]. In severe situations, it results in retinal detachment, which leads to cause a total blindness. Any person who has had diabetes type-1 or type-2 is susceptible to developing DR. Although this disease has potentially fatal implications, people with diabetes can lead normal lives with the right care, medicine, and therapy [3]. If diabetes is not treated quickly, it may worsen a person's vision. It is crucial to make a diagnosis of this condition as soon as possible in order to fully eradicate it and preserve the vision of those who are suffering from diabetic retinopathy. If diabetes-related retinal disease is treated, many people could avoid going blind. It is now crucial to develop a system that automatically identify this issue and generates the best result to the ophthalmologist to provide better treatment [4, 5]. Therefore, an automated grading system for DR has been proposed in this work. It eliminates a lot of manual labour and, with the aid of image processing and ML, which has ability to predict the accurate results from massive datasets.

Several research has been proposed to predict the DR in early phase, which is listed below. In [6] authors have proposed a heuristic-based data enhancement strategy that involves the creation of Neovessel (NV) includes structures to make up for the dearth of PDR cases in DR considered datasets. The data augmentation strategy has been validated on several datasets and enhances the representation's ability to find NVs. However, the existence of light artefacts, which cause colour aberrations, is the main cause of the NV ascribed colours occasionally not being highly accurate. In [7], an innovative Siamese-like Convolutional Neural Network (CNN) framework is developed using a transfer learning method. The aforementioned model takes as inputs binocular fundus images and trains the ability to correlate them in order to produce a forecast. However, comparatively more samples are incorrectly classified. It might be concluded that it is harder to accurately identify DR in its early phases. The Internet of Things Deep Learning - DR Detection (IoTDL-DRD) approach is described in [8] and uses IoT devices for gathering data that is then transferred to a remote server in the cloud for processing. Here, an efficient DR diagnosis is achieved by using an LSTM-based classifier. Although the process is terminated, it still completes the window's final index. Measurement of intergrader variance is used in [9] to analyse the annotator level of DR rating. The inter-grader variance of the existence of DR related features is assessed using cosine correlation, and the intergrader variance of DR severity ratings is evaluated using quadratic weighted Cohen's kappa. In consideration of these findings, a two-step technique may be used to diagnose the seriousness of DR as well as the presence of DR-related characteristics. However, since they seem to be uncommon in the dataset, this study excludes vitreous or preretinal haemorrhage and traction retinal detachment from evaluation. A unique method for identifying DR using transfer learning, incorporating intra- and inter-domain alignment, is described in [10] as Graph Adversarial Transfer Learning (GATL). The only drawback of GATL is that it is unable to account for precise categorization of lesions. GATL is able to identify with excellent precision when a lesion has developed or not due to the small size and resemblance of DR lesions; however, additional analysis is needed to assess the severity of illness.

Thus, the PNN classifier is implemented to forecast the DR in early phases with high precision. The noises are removed from the original image with the adoption of bilateral filter. Here, the segmentation is accomplished by SFCM method for further process. Following the segmentation, the feature extraction and selection are performed by GLCM and GA respectively. Finally, the proposed PNN classifier effectively diagnoses DR from the input retinal image.

II. RELATED WORKS

1. **Khan Zubair *et al* (2021)** have proposed to categorize the DR's numerous phases with the smallest learnable variables possible in order to hasten model convergence and training. The findings from experiments establish that the advised method outperforms state of the art methodologies in terms of accuracy and efficient use of computer resources. However, it necessitates certain additional beneficial adjustments to the architecture of the current model along with certain preprocessing methods. It is necessary to examine whether these adjustments impact the operation of a model on the organization of DR's phases, particularly the early ones.
2. **Qummar Sehrish *et al* (2019)** have demonstrated to use the open-access Kaggle dataset of retinal pictures for training a group that includes five deep CNN networks to represent the rich features and develop the categorization for several stages of DR. The results of the experiments indicate that, in contrast to the state of the art approaches on the identical Kaggle dataset, the proposed framework identifies each phase of DR. But, some of trained specialized models are required for particular phases to boost the initial stages precision, and then the results are to be combined to improve the early phases' accuracy.
3. **Pour Asra Momeni *et al* (2020)** have explained a novel DR monitoring technique that employs the Contrast Limited Adaptive Histogram Equalisation (CLAHE) technique as a preprocessing step to enhance the quality of pictures and consistently equalise intensities. It also considerably lowers costs and is able to employ for monitoring DR despite the requirement for an expert. Although EfficientNet-B0 to B4 significantly decreases the image size, valuable data in the image is eliminated during processing.
4. **Qiao Lifeng *et al* (2020)** have proposed a CNN methods that incorporate Deep Learning (DL) as an important part and are enhanced by Graphics Processing Units (GPUs), to evaluate the possibility of microaneurysms in fundus images. These methods are going to carry out medical picture identification and segmentation with outstanding efficacy and minimal inference delay. But, simplifying the evaluation of all qualities is inappropriate.
5. **Abdelsalam Mohamed M (2021)** have presented a cutting-edge process for DR early discovery that is based on multifractal geometries. For the purpose of identifying early Non-PDR (NPDR), Macular Optical Cherenche Tomography Angiography (OCTA) photographs are analyzed. This method also makes it simple to categorize later stages of DR conditions that influence the spread of neovascularization. However, it is unable to diagnose a medical picture numerically on its own.

III. PROPOSED SYSTEM

The fluids form in several forms of retinal lesions caused by DR, which is caused by blood spilling from vessels that are not natural in origin. The proposed technique for detecting DR using PNN classifier is shown conceptually in Figure 1.

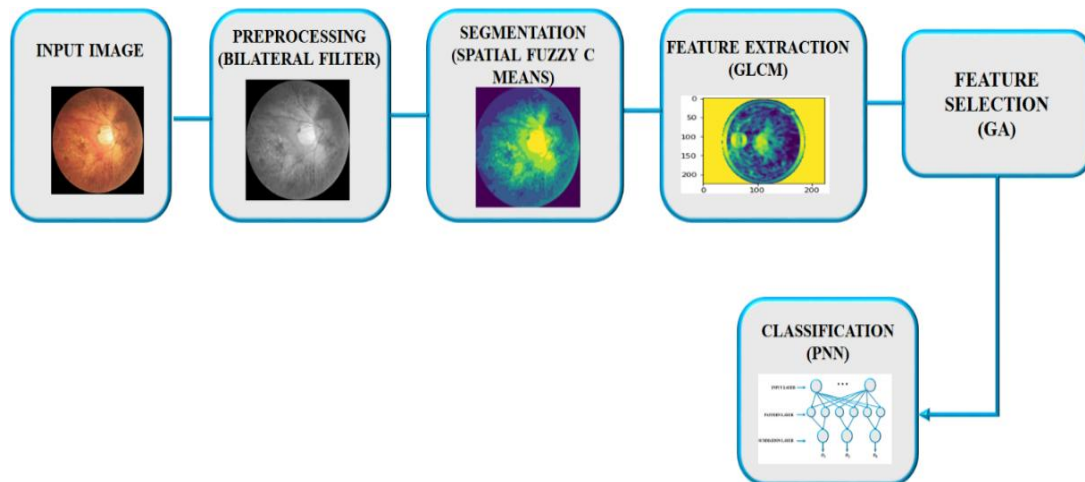


Figure 1: Diagnosis of Diabetic Retinopathy using PNN Classifier

Initially, the retina image is subjected into the bilateral filter for preprocessing, where an unidentified signal is projected by using a related signal as input, then filtered to yield the estimate. Based on the distribution of determined pixel values, the distortion-free image is then segmented by a SFCM algorithm that determines an ideal threshold automatically. Consequently, feature extraction is implemented by GLCM to extract second order statistical features of texture for estimating motion of images. Here, the process is developed with the help of feature selection-based GA. By choosing the optimum parameters and eliminating the redundant and irrelevant ones, it also expands the approach's predictive capability. As a final step, the image is classified using PNN via minimal preprocessing and convolution operations and the efficient detection of diabetic retinopathy in eye is accomplished.

1. Preprocessing of Input Image Image Using Bilateral Filter: In this research the image is preprocessed through the use of bilateral filter approach. Bilateral filtering method smooth's the images while preserving edges by applying a nonlinear collection of variables from neighbouring images. The goal of bilateral filtering is to achieve over the entire range of images that conventional filters perform in that region. A pixel is capable of being similar to a different pixel by occupying the same location data, or it also be similar to another pixel by sharing values that are perhaps visually relevant. Likewise the terms "close" to and comfortable denote proximity in the domain and range, correspondingly. Traditional filtering is a type of domain filtering that encourages proximity by assessing the amount of pixels using coefficients which reduce with range. Range filtering normalised image values are achieved by combining image information with weights that decrease with differentiation. Variety filters are nonlinear because their parameters vary according to the clarity of the image. It never become complicated to analyse than standard non-separable filters. The combined operation of domain and range filtering is referred to as bilateral filtering.

$$h(y) = k_d^{-1}(y) \int_{-\infty}^{\infty} \int_{-\infty}^{\infty} f(\varepsilon) c(\varepsilon, y) d\varepsilon \quad (1)$$

The possibility that input and output pictures are likely multiband is emphasized by choice of a letters bold typeface f and h , the geometric distance between an adjacent location and the neighbourhood centre x is determined by the expression $c(\varepsilon, y)$. The expression that follows is obtained if low pass filtering is to be used for preserving the low pass data,

$$k_d(y) = \int_{-\infty}^{\infty} \int_{-\infty}^{\infty} c(\varepsilon, y) d\varepsilon \quad (2)$$

Whenever, the shift-invariant is called as filtering, the constant value is represented by k_d , and vector variance that influences $c(\varepsilon, y)$ is $(\varepsilon - y)$. As a result, the similarity function s is still operating in the domain of f , whereas the proximity function c is presently operating in the domain of f . From equation (2) the adjusted normalizing constant is,

$$k_r(y) = \int_{-\infty}^{\infty} \int_{-\infty}^{\infty} s(f(\varepsilon), f(y)) d\varepsilon \quad (3)$$

In contrast to the closeness function c , the normalisation function s is dependent on the image f . If the information shared by the function s simply alters according to the difference $f(\varepsilon), f(y)$, and then it is neutral (y) . The related range filtering and domain that assures concurrent photometric localization and geometrics known as bilateral filtering. Combination filtering is described as follows:

$$h(y) = k^{-1}(y) \int_{-\infty}^{\infty} \int_{-\infty}^{\infty} f(\varepsilon) c(\varepsilon, y) s(f(\varepsilon), f(y)) d\varepsilon \quad (4)$$

With the normalization,

$$k(y) = \int_{-\infty}^{\infty} \int_{-\infty}^{\infty} c(\varepsilon, y) s(f(\varepsilon), f(y)) d\varepsilon \quad (5)$$

Thus, the Bilateral filter effectively analyses the input images and provides an absence of noise output image.

- 2. Image Segmentation Using SFCM Algorithm:** Following image pre-processing, a SFCM clustering method is implemented to segment the images, allowing the afflicted blood vessels to be identified. The high correlation of adjacent pixels is one of an image's key properties. In other words, there is a high likelihood that these adjacent pixels are part of the same cluster because they have similar feature values. Although this spatial link is crucial for clustering, a basic FCM method does not use it. A spatial function has been defined as follows in order to utilise the spatial information:

$$h_{ij} = \sum_{k \in NB(x_j)} U_{ik}, \quad (6)$$

where $NB(x_j)$ denotes a rectangular window in the spatial domain that is centred on the pixel x_j . This task is performed entirely inside a 5×5 window. The spatial function h_{ij} indicates the likelihood that pixel x_j corresponds to i th cluster, just like the membership function implies. If most of the pixels in a given neighbourhood are members of identical clusters, the spatial information of that pixel for that cluster is big. The inclusion of the spatial value into the function of membership is described as follows:

$$u'_{ij} = u_{ij}^p h_{ij}^q / \sum_{k=1}^c u_{kj}^p h_{kj}^q \quad (7)$$

where the parameters p and q regulate the respective weights of the two functions. In a homogeneous area, the spatial functions only support the initial membership, and the clustering outcome is unaffected. However, this algorithm de-weights and labels the neighboring pixels of the noisy cluster for the noisy pixel. As an outcome, spurious blobs or incorrectly classified pixels from noisy areas are adjusted with simplicity. The term " $SFCM_{p,q}$ " refers to the spatial FCM with parameters p and q . Note that the traditional FCM and $SFCM_{1,0}$ are the same.

Every stage of the clustering involves two passes. For determining the spectral domain membership function, the initial pass is accurately the same as in normal FCM. The second pass involves mapping each pixel's membership information to the spatial domain and computing the spatial function using that information. The updated membership that incorporates the spatial function is added to the FCM iteration. When the largest changes among 2 cluster centres at two subsequent iterations is smaller than a predetermined threshold value ($= 0.02$), the iteration is terminated. Defuzzification is used for allocating every pixel to a certain cluster for that the membership is highest after convergence. As a result, the pre-processed raw image is successfully segmented by the SFCM methodology, which is more suitable for noisy images where it is difficult to identify the edges.

3. Feature Extraction using GLCM Method: The presence of features in images contributes to the development of increased precision, but a high number of features increases process complexities, consumption of time, memory waste, etc. This could result in an issue with overfitting. To solve this problem, GLCM is used, a feature extraction technique of second order that involves the utilization of a matrix of co-occurrence to indicate the neighbour relationships between picture pixels for various directions and spatial ranges. Following includes a list of the features that are extracted and used for feature selection,

- **Energy:** It provides information about the concentration size of the pair with a specific grey intensity in the co-occurrence matrix.

$$Energy = \sum_{i=1}^L \sum_{j=1}^L q(i,j)^2 \quad (8)$$

- **Contrast:** It is determined by, and it describes the size of the scattering of inertia moments or changes in picture matrices.

$$Contrast = \sum_i^L \sum_j^L |i - j|^2 q(i,j) \quad (9)$$

- **Homogeneity:** The term "homogeneity" refers to the way homogeneous an image is on a grey scale level and is defined as,

$$Homogeneity = \sum_{i=1}^L \sum_{j=1}^L \frac{q(i,j)^2}{1+(i-j)^2} \quad (10)$$

- **Dissimilarity:** Dissimilarity is defined as the measurement of a grey level image's variations.

$$Dissimilarity = \sum_k \sum_l P(k,l) |k - l| \quad (11)$$

- **Correlation:** Correlation is defined as the calculated value of the linear dependence of the grey currency matrix with respect to the picture and is given by,

$$Correlation = \sum_{i=1}^L \sum_{j=1}^L \frac{(i-\mu_i)(j-\mu_j)p(i,j)}{\sigma_i\sigma_j} \quad (12)$$

Therefore the segmented features are efficiently separated from the image implementing GLCM approach and further fed to the feature selection process.

4. Feature Selection using Genetic Algorithm: The process of choosing the least amount of features required for precise prediction (classification) is known as feature selection. This is accomplished by eliminating unnecessary and irrelevant features. Redundant features are those that offer no more information beyond the ones that are currently being used, while irrelevant features offer no information that is relevant in any situation. Improved classifier performance and a clearer understanding of the underlying process that produced the data are two advantages of feature selection. Nevertheless, it takes a lot of time to execute a network search of the classification variable every time a fresh subset feature is chosen. Here, the GA, which once allowed for the exploration of the ideal subset feature and classifier variables to take place concurrently—is presented as a solution to this issue. The pre-selection of the kernel function type is the only prerequisite. Figure 2 shows a flow chart outlining the design of the system. Each feature is normalised to have a mean of zero and a standard deviation of one. This approach had been carried out individually for the linear, polynomial kernel functions and Radial Basis Function (RBF), because the kernel function type had already been determined. Following is a description of the key steps:

- As an initial location, use the box from Figure. 2 designated population. A population of chromosomes is initialised at random and a feature subset have been detected on each chromosome.
- The following approach is adopted to assess every chromosome in the population on an individual basis. The fitness function used to assess the chromosome is calculated from a number of chosen features.
- To determine whether the stoppage requirements have been met, the fitness functions of every chromosome in the population are examined. The terminating criteria have been adjusted to the highest fitness function attainable. The process stopped if it achieved that point; else it moved on to the genetic operations.
- The following generation (new population) has been generated through genetic procedures. This is achieved by initially choosing the best chromosomes as parents, followed by the production of offspring (a new population) by crossover and mutation.

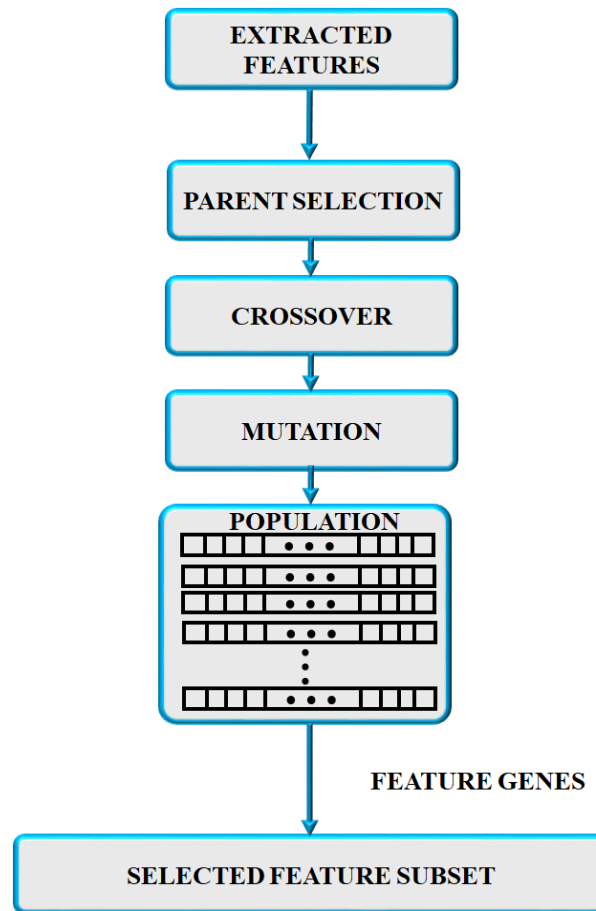


Figure 2: Flowchart of Feature Selection using GA

When the stopping condition had been satisfied or the predetermined maximum number of generations is attained, steps (2) through (4) are carried out recursively. As an outcome, the image's features are determined by employing a GA technique and then subject into the proposed PNN classifier.

- 5. Classification Using PNN Classifier:** The training phase and the testing phase are the two key stages of the classification procedure. The known information are provided in the initial step of training, and then certain data sets are employed in the following phase to train the proposed system. The clustered classifier is implemented to execute classification after training in the subsequent stage of the testing phase, which involves the provision of unidentified data. This stage involves converting the features from the previous procedure into feature vectors. The PNN classifier produces precise predictions with rapid convergence, and its parallel design helps significantly in producing the best results. The preparation step's calculation heap is transferred to the evaluation stage, which is PNN's primary identifying feature. PNN contains four layers: input, pattern, summation, and output. Multiple categories are supported by PNN. The underlying layer establishes the separation among the data vector and the training vector at the time that the information is given to the structure. The next layer combines up all of these promises for each category of sections to produce a vector of probability at the output. Finally, an exchange operation at the output of the following layer takes the determined of these probabilities and outputs 1 for this class and 0 for all other classes.

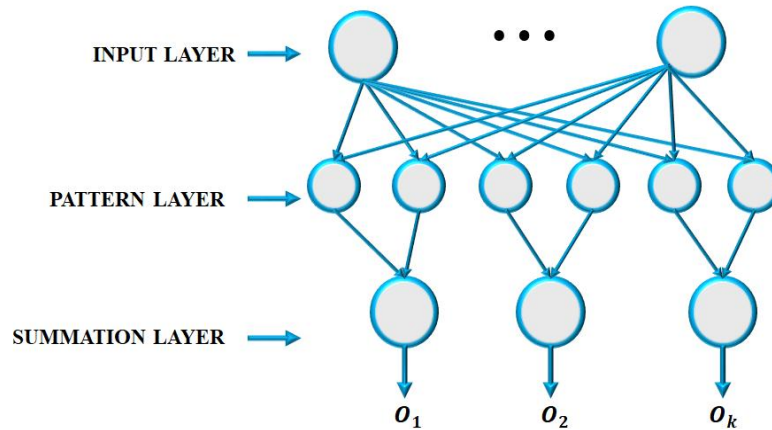


Figure 3: PNN Classifier

As an outcome, the enlarged version of the radial base transfer function serves as the vector class input of the PNN with an optimal level of precision in the possibility category. In Figure 3, the PNN structure is displayed. Every training variable is fixed on by radial and circular gaussian functions in PNN. A vector's likelihood of belonging to a particular class is expressed as,

$$f_i(x) = 1/2\pi^{P/2}\sigma^P M_i \sum_{j=1}^M e^{-(x-x_{ij})^T(x-x_{ij})/2\sigma^2} \quad (13)$$

When the number of classes is i , the number of forms is j , the test vector is x , the quantity of training data for class i is p , the value of the smoothing factor is r , and the σ is probability density function for class i is given as x_{ij} . The classification determination is decided by,

$$d(x) = C_i \text{ if } : f_i(x) > f_k(x) \text{ for } k \neq i(2) \quad (14)$$

where i is the C_i 's class.

Every derived feature value from the test picture is changed into each instance of training feature value if the value of the resulting feature value corresponds to any training amount. The illustration records the likelihood of the specific training example.

IV. RESULTS AND DISCUSSION

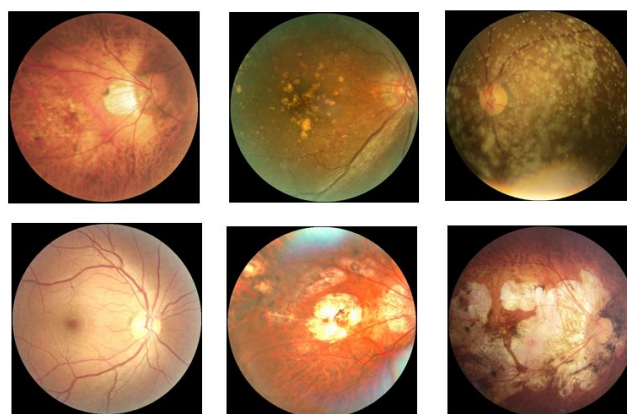


Figure 4: Original Image

The software platform Python is used to execute the DR (Diabetic Retinopathy) Detection using Image Processing technique proposed in this paper. The DR Finding utilizing Image Processing Technique yields the simulated results. This method uses procedures that allow for the detection of affected DR in the fundus image but not of DR in the healthy fundus picture. Figure 4 represents the original DR images.

1. Output of Pre-Processing

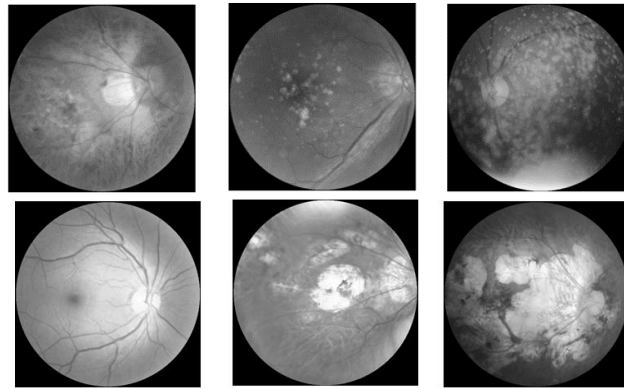


Figure 5: Preprocessed by Using Bilateral Filter

An image has been modified using the image filler approach. It is used on the fundus image to preserve certain features while removing others. The main goal of preprocessing is to raise the DR images' quality and additionally, it aids in the improvement of several aspects of DR images, such as boosting the visual appeal of DR images, eliminating unnecessary noise and undesirable background factors, enhancing the inner part of the region, and maintaining its edges. Thus, the proposed Bilateral filter improves the clarity of the DR images with reduced noise.

2. Output of Segmentation

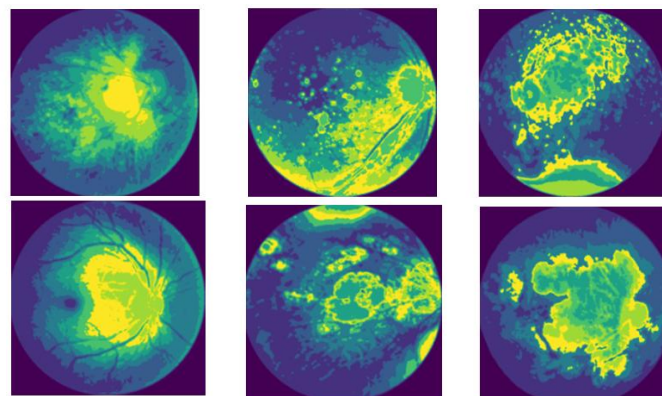


Figure 6: Segmented by using SFCM

To make a picture easier to analyse, it needs to be divided into several segments, a process known as image segmentation. It is meant to locate different objects and limits, such as lines, circles, and curves. Whether a particular pixel is a vessel or not is

determined by the segmentation of the image (retinal vessel segmentation). Here, the segmented retinal fundus image has been generated using the SFCM method, and the outcome is shown in the Figure shown above. It is put up against the traditionally discovered vascular network and clearly demonstrates effective outcomes.

3. Feature Extraction

Table 1: Feature Extraction

No.	Feature extraction				
	Homogeneity	Correlation	Dissimilarity	Energy	Contrast
1	0.54100	0.99360	1.87199	0.18908	46.4553
2	0.48130	0.98865	2.48282	0.19840	50.8757
3	0.52577	0.91743	2.04726	0.18724	28.8544
4	0.44736	0.99484	3.05427	0.19623	91.7448
5	0.47142	0.99185	2.70161	0.19105	90.8891
6	0.45294	0.99595	3.10074	0.19326	40.2479

The collection of data for the extraction of characteristics which includes homogeneity, energy, dissimilarity contrast, and correlation are shown in the aforementioned table. The results have been acquired using the GLCM technique on datasets for both healthy and diabetic retinopathy. To pick appropriate features for the classifier's development is the main goal of feature selection. In this work, the GA-based feature selection approach is used; it has the benefits of quicker training times, reduced overfitting, and avoidance of the dimensional problem while still producing the model. To improve the features of DR lesions even more, the GA is utilised. By picking the best significant parameters and removing the terminated and insignificant ones, it also improves the methods capability to anticipate outcomes. Image classification is made possible by the segmented region produced through feature extraction and selection and the recovered parameters. Finally, with the utilization of GA, contrast, energy and homogeneity features are selected.

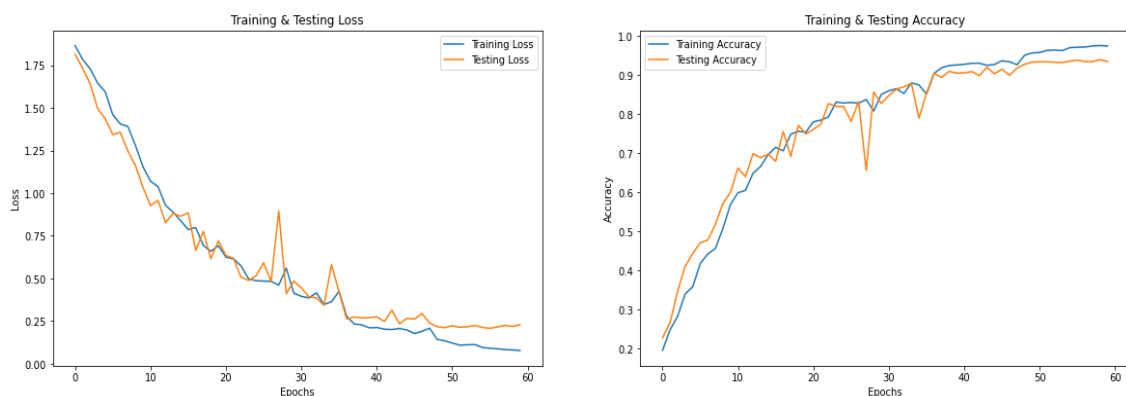


Figure 7: Accuracy & Loss of PNN Classifier

Figure 7 denotes the accuracy and loss of testing and training period of PNN classifier. From the graph is it clear that the proposed PNN classifier has improved

accuracy loss with low testing & training loss. As a result, the proposed technique efficiently identifies DR in coloured fundus images.

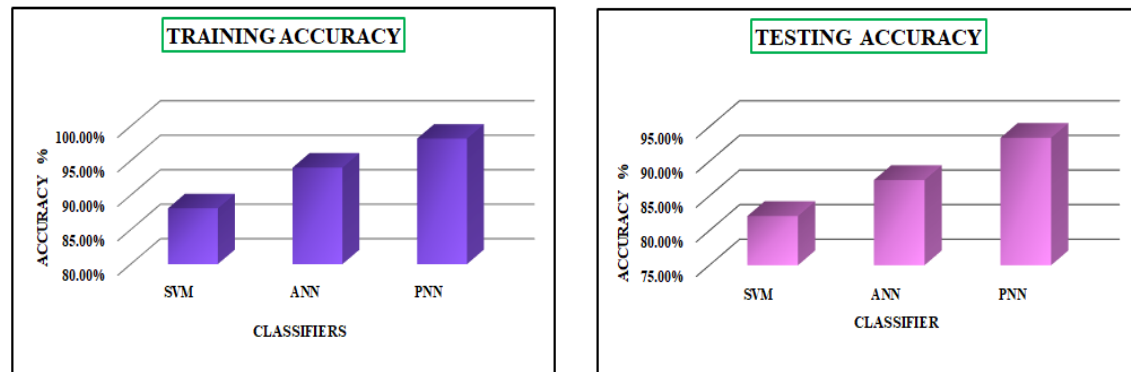


Figure 8: Comparison Analysis of Classifier Accuracy

Figure 8 indicates comparison analysis of classifiers training and testing accuracy. From the obtained results, it is evident that, the proposed PNN classifier achieves highest testing and training accuracy 93.4% & 98.2% correspondingly.

Table 2: Strategies for Comparative Analysis

Approaches	Sensitivity	Accuracy	Specificity	Dataset Images
Entropy CNN classification [16]	73.2	86.1	93.81	21,123
K-nearest neighbor (KNN)+ Fractal analysis [17]	-	89.17	-	120
CNN+Image processing [18]	94	97	98	400
Deep neural network (DCNN) [19]	90	98	96	294
DNN-(PCA)-Firefly [20]	92	97	95	1151
SVM-RBF [21]	97.3	94.3	87.0	105
PNN (proposed)	98.1	98.5	98.7	550

Several classification methods have been provided together with their effectiveness as indicators, as shown in Table 2. Deep neural networks are employed in two methodologies, including Principle Component Analysis (PCA) using Firefly [20] and [19]. [16], [18], two research based on CNN. K-nearest neighbour (KNN) and fractal analysis were both employed in another study [17]. All of the approaches' precision, specificity, and sensitivity have been assessed. From the analysis, it is clear that the proposed PNN classifier outperforms than other methods.

Table 3: Measurements of SNR, RMSE, PSNR and MSSIM achieved by various Noise Elimination Techniques

Techniques	SNR (Signal-to-Noise Ratio)	PSNR (Peak Signal-to-Noise Ratio)	RMSE (Root Mean Square Error)	MSSIM (Multi Scale Structural Similarity)
Bilateral Filter	20.3196	77.0421	0.0012	0.993
Wiener Filter	15.8176	24.2345	245.26	0.635
Median Filter	16.2601	16.2601	213.32	0.628

Based on the outcomes in the Table 3. It has to be noted that the proposed bilateral filter strategy offers better MSSIM, SNR, and PSNR values as well as low RMSE values when compared to other two filters, such as the wiener filter and median filter. This indicates that it maintain the image features after the eliminating process.

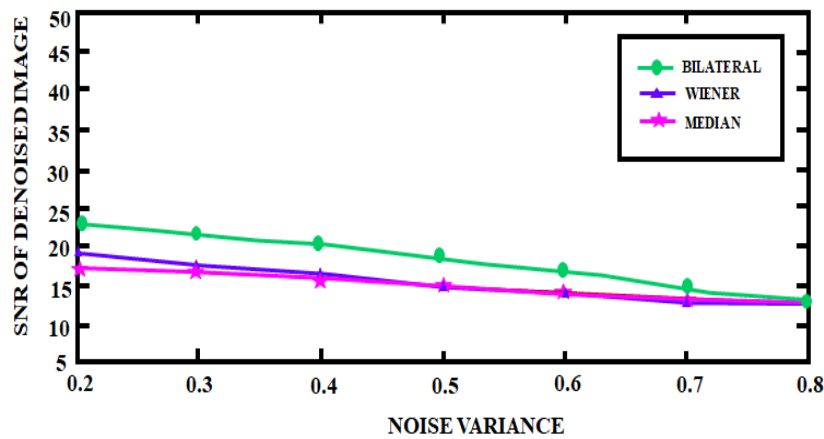


Figure 9: Effectiveness of Denoising Images Under Noise SNR Calculated in Comparison to Various Noise Values

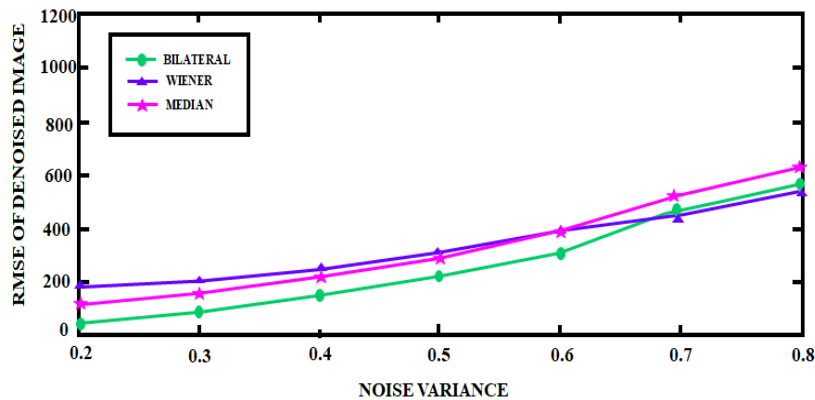


Figure 10: Effectiveness of Image Denoising under Noise RMSE calculated in Comparison to Various Noise Values

Figure 9 shows that compared to other noise reduction techniques, the bilateral filter method produces a considerable SNR gap. In regard to RMSE, Figure 10 demonstrates that the bilateral filter strategy also yields the minimum value of RMSE.

V. CONCLUSION

Blindness is a result of diabetic retinopathy, a condition that affects the blood vessels of the retina. To identify this severe condition, colored fundus injections are frequently utilized. It is tedious and prone to mistakes for clinicians to manually analyse the aforementioned images. Thus, the present research suggests an automated classification strategy to assess the severity of DR. The first step in the evaluation of retinal images is the application of the bilateral filter, which also functions as a preprocessing tool. By protecting the features of the retinal arteries, it successfully reduces image noise and creates a better-quality image for future processing. Following the removal of background noise, segmentation is carried out using SFCM clustering, which combines spatial information into the membership function for clustering and produces the optimal segmented output. The results demonstrate that it is feasible to diagnose both DR severity levels and DR related features in fundus images with good performance. After segmentation, features are extracted and chosen using GLCM and GA, correspondingly, and then a PNN classifier is used to determine the severity of DR. The findings demonstrate the remarkable accuracy and effectiveness of the proposed approach for detecting DR using retinal fundus images

REFERENCES

- [1] M. Ghazal, S. S. Ali, A. H. Mahmoud, A. M. Shalaby and A. El-Baz, "Accurate Detection of Non-Proliferative Diabetic Retinopathy in Optical Coherence Tomography Images Using Convolutional Neural Networks," in *IEEE Access*, vol. 8, pp. 34387-34397, 2020, doi: 10.1109/ACCESS.2020.2974158.
- [2] J. Xu et al., "Automatic Analysis of Microaneurysms Turnover to Diagnose the Progression of Diabetic Retinopathy," in *IEEE Access*, vol. 6, pp. 9632-9642, 2018, doi: 10.1109/ACCESS.2018.2808160.
- [3] Usman and K. A. Almejalli, "Intelligent Automated Detection of Microaneurysms in Fundus Images Using Feature-Set Tuning," in *IEEE Access*, vol. 8, pp. 65187-65196, 2020, doi: 10.1109/ACCESS.2020.2985543.
- [4] K. Shankar, Y. Zhang, Y. Liu, L. Wu and C. -H. Chen, "Hyperparameter Tuning Deep Learning for Diabetic Retinopathy Fundus Image Classification," in *IEEE Access*, vol. 8, pp. 118164-118173, 2020, doi: 10.1109/ACCESS.2020.3005152.
- [5] Y. Jiang, N. Tan, T. Peng and H. Zhang, "Retinal Vessels Segmentation Based on Dilated Multi-Scale Convolutional Neural Network," in *IEEE Access*, vol. 7, pp. 76342-76352, 2019, doi: 10.1109/ACCESS.2019.2922365.
- [6] Araújo, Teresa, et al. "Data augmentation for improving proliferative diabetic retinopathy detection in eye fundus images." *IEEE access* 8 (2020): 182462-182474.
- [7] Zeng, Xianglong, et al. "Automated diabetic retinopathy detection based on binocular siamese-like convolutional neural network." *IEEE access* 7 (2019): 30744-30753.
- [8] Palaniswamy, Thangam, and Mahendiran Vellingiri. "Internet of Things and Deep Learning Enabled Diabetic Retinopathy Diagnosis Using Retinal Fundus Images." *IEEE Access* 11 (2023): 27590-27601.
- [9] Wang, Juan, Yujing Bai, and Bin Xia. "Feasibility of diagnosing both severity and features of diabetic retinopathy in fundus photography." *IEEE access* 7 (2019): 102589-102597.
- [10] Hu, Jingbo, et al. "Graph Adversarial Transfer Learning for Diabetic Retinopathy Classification." *IEEE Access* 10 (2022): 119071-119083.
- [11] Khan, Zubair, et al. "Diabetic retinopathy detection using VGG-NIN a deep learning architecture." *IEEE Access* 9 (2021): 61408-61416.
- [12] Qummar, Sehrish, et al. "A deep learning ensemble approach for diabetic retinopathy detection." *Ieee Access* 7 (2019): 150530-150539.

- [13] Pour, Asra Momeni, et al. "Automatic detection and monitoring of diabetic retinopathy using efficient convolutional neural networks and contrast limited adaptive histogram equalization." *IEEE Access* 8 (2020): 136668-136673.
- [14] Qiao, Lifeng, Ying Zhu, and Hui Zhou. "Diabetic retinopathy detection using prognosis of microaneurysm and early diagnosis system for non-proliferative diabetic retinopathy based on deep learning algorithms." *IEEE Access* 8 (2020): 104292-104302.
- [15] Abdelsalam, Mohamed M., and M. A. Zahran. "A novel approach of diabetic retinopathy early detection based on multifractal geometry analysis for OCTA macular images using support vector machine." *IEEE access* 9 (2021): 22844-22858.
- [16] G.-M. Lin, M.-J. Chen, C.-H. Yeh, Y.-Y. Lin, H.-Y. Kuo, M.-H. Lin, M.-C. Chen, S. D. Lin, Y. Gao, A. Ran, and C. Y. Cheung, "Transforming retinal photographs to entropy images in deep learning to improve automated detection for diabetic retinopathy," *J. Ophthalmol.*, vol. 2018, pp. 16, Sep. 2018, doi: 10.1155/2018/2159702.
- [17] D. W. Safitri and D. Juniati, "Classification of diabetic retinopathy using fractal dimension analysis of eye fundus image," in *Proc. AIP Conf.*, 2017, Art. no. 020011, doi: 10.1063/1.4994414.
- [18] D. J. Hemanth, O. Deperlioglu, and U. Kose, "An enhanced diabetic retinopathy detection and classification approach using deep convolutional neural network," *Neural Comput. Appl.*, vol. 32, no. 3, pp. 707-721, Feb. 2020, doi: 10.1007/s00521-018-03974-0.
- [19] N. Ramachandran, S. C. Hong, M. J. Sime, and G. A. Wilson, "Diabetic retinopathy screening using deep neural network," *Clin. Experim. Ophthalmol.*, vol. 46, no. 4, pp. 412-416, May 2018, doi: 10.1111/ceo.13056.
- [20] T. R. Gadekallu, N. Khare, S. Bhattacharya, S. Singh, P. K. R. Maddikunta, I.-H. Ra, and M. Alazab, "Early detection of diabetic retinopathy using PCA-firefly based deep learning model," *Electronics*, vol. 9, no. 2, p. 274, Feb. 2020, doi: 10.3390/electronics9020274.
- [21] N. Eladawi, M. Elmogy, F. Khalifa, M. Ghazal, N. Ghazi, A. Aboelfetouh, A. Riad, H. Sandhu, S. Schaal, and A. El-Baz, "Early diabetic retinopathy diagnosis based on local retinal blood vessel analysis in optical coherence tomography angiography (OCTA) images," *Med. Phys.*, vol. 45, no. 10, pp. 4582-4599, Oct. 2018, doi: 10.1002/mp.13142.